Adhesion Measurement of Interfaces Between Gelatin and Poly(ethylene terephthalate) Using Microscratch Technique

Chi-An Dai,[1] Chih-Chien Liao,[1] Tai-An Tsui,[1] Hao-Ching Chien,[1] Ming-Wei Liu[2]

[1]*Department of Chemical Engineering and Institute of Polymer Science and Engineering, National Taiwan University, Taipei 106, Taiwan*
[2]*Taiwan Adventist Hospital, Taipei 105, Taiwan*

Received 24 August 2004; accepted 28 May 2005
DOI 10.1002/app.22697
Published online in Wiley InterScience (www.interscience.wiley.com).

ABSTRACT: A microscratch technique was used to evaluate the adhesion between interfaces of a gelatin coating and poly(ethylene terephthalate) (PET) film. The interface was reinforced by nitrogen plasma treatment on the PET surface and subsequently by heat treatment of each gelatin/PET sample to promote interactions at the interface. In the microscratch test, a normal load controlled conical stylus with 50-μm radius tip was drawn over the gelatin coating surface under a continuously increasing normal load until failure occurred in the sample. Optical microscopy and depth profiling of the scratch track were used to detect failure and the failure mechanism. The critical normal load (F_c) was defined as when gelatin detached from the PET substrate or when a complete removal or plowing of the gelatin coating on the PET substrate occurred. With increasing plasma treatment time and heating treatment temperature, the F_c for both debonding and coating removal increased, which showed that both failure mechanisms are related to the adhesion. Different thicknesses of the gelatin coatings were also prepared under the same plasma and heat treatment conditions. It was found that the F_c increased with increasing coating thickness. The result demonstrated that both failure mechanisms depended on the plastic deformation of the coating and substrate. The F_c for coating detachment increased linearly with increasing coating thickness whereas the F_c for coating removal increased sharply with increasing thickness. Annealing temperatures ranging from 20 to 80°C exhibited a strong effect on the F_c, which increased with increasing annealing temperature. These results demonstrate that the microscratch technique can be used to access interfacial adhesion and that the F_c is a qualitative parameter for the evaluation of adhesion strengths. © 2005 Wiley Periodicals, Inc. J Appl Polym Sci 99: 1960–1974, 2006

Key words: gelatin; poly(ethylene terephthalate); scratch; adhesion; plasma treatment

INTRODUCTION

Thin polymeric coatings are widely used to modify various bulk properties of their substrates, including chemical, mechanical, protective, aesthetic, electromagnetic, and biocompatible properties.[1] For example, in order to improve the biocompatibility of artificial vessels made of poly(ethylene terephthalate) (PET), a thin-film gelatin layer is often coated.[2,3] Gelatin, which is derived from collagen via a hydrolysis process, is often considered as a biocompatible and economical natural material.[4,5] However, the interface between PET and many synthetic or natural polymeric materials is rather weak. A small excess force can cause delamination between the coated layer and PET, which could severely affect the performance of the device in service. Therefore, finding a solution to improve the interfacial adhesion between two incompatible polymers has long been a critical issue and an actively researched topic.[6] Moreover, many traditional methods measure interfacial adhesion between two bulk materials (e.g., peel test, wedge test, etc.) and are limited in their thin-film and multilayer geometry requirements, with thicknesses ranging from submicrons to several 10s of microns. Therefore, there are great demands to explore new methods of measuring thin-film adhesion.[7]

Indentation and scratch techniques are attractive methods to evaluate the mechanical properties and adhesion of thin coatings because they often require no additional sample preparation for testing.[8–11] The process of indentation involves contact between a material of interest and a hard indenter under increasing normal load. The stress analysis around an indenter in a semi-infinite material was first studied by Hertz[12] and later extensively examined by Johnson for indenters of different geometries.[13] For a homogeneous semi-infinite material, Hertzian elastic contact theory shows that a complete stress field in the material around an indenter can be obtained. In particular, it also shows that the maximum Von Mises shear stress

Correspondence to: C.-A. Dai.
Contract grant sponsor: National Science Council; contract grant number: NSC91-2216-E-002-015.
Contract grant sponsor: Ministry of Economics of Taiwan.

occurs at a depth roughly one-half of the indenter radius beneath the contact surface. In scratch testing an indenter is typically drawn across the sample surface under progressively increasing normal load. Failure in the coating may occur at a particular load, which is often defined as the critical load (F_c). Many studies have found that the F_c increases with increasing coating thickness and hardness.[14–16] The mode of failure due to scratching depends on both the cohesive and adhesive properties of coatings and substrate materials.

The stress field in the layered material around an indenter during a scratch test can be qualitatively treated as the combination of the stress field induced by the normal and sliding contact between an indenter and the layered material. O'Sullivan and King studied the elastic sliding contact stress field around a spherical stylus of a coating/substrate material.[17] When the elastic property of the coating was different from that of the substrate, they found that there was a discontinuity of the Von Mises stress at the coating/substrate interface. With increasing frictional force, this difference in the stress discontinuity became greater. The stress discontinuity may have a significant effect on the adhesion measurement because coatings may debond from substrates as the horizontal in-plane shear stress exceeds the shear strength of the interface. O'Sullivan and King's[17] result also showed that the maximum Von Mises stress (which is located beneath the contact surface in pure indentation testing) moves closer to the contact surface between the stylus and the coating in scratch testing. During scratch testing, an in-plane tensile stress behind the stylus and an in-plane compressive stress ahead of the stylus develop. The tensile and compressive stresses can cause fracture of the coating surface, which affects the scratch morphology and the adhesion measurement.

Many scratch adhesion testing studies have been reported.[18–20] However, most studies have concentrated on scratch testing on harder coating/substrates materials, for example, ceramics or metals. In polymeric coating/substrate systems, large plastic deformation can be generated not only in polymer coating but also in polymer substrates. Additional shear stress at the interface is produced because of the local bending of the coating/substrate interface by the indenter. The purpose of this research is to explore the possibility of using scratch testing as a tool to evaluate adhesion strength. We also explore the possibility of using scratch testing to measure adhesion on a polymer coating/polymer substrate system.

EXPERIMENTAL

Scratch adhesion test

The scratch adhesion measurement was performed using commercial equipment (Micro Scratch Tester) supplied by CSEM Instruments of Switzerland. The operation of the scratch test can be treated as a combination of a normal indentation motion and a horizontal sliding motion of the stylus tip. The Micro Scratch Tester is a normal load controlled device and the normal indentation operation is carried out by the stylus assembly in the device placed closely above the sample surface. A conical diamond stylus (Rockwell C diamond) with an apical angle of 120° and tip radius of 50 μm was used as the probe to scratch the samples in all of the tests. Scratches were made by moving a precision translation sample stage while the stylus was drawn across the sample surface with increasing normal load and corresponding horizontal load. The stylus is attached to a depth sensor that records the vertical position (depth) of the stylus tip relative to the coating surface. Before each scratch test, a topographic scan (prescan) of the sample surface was set up to check any tilting or roughness of the sample at a minimal normal load (0.03 N) and at a horizontal speed of 5 mm/min. Upon completing the prescan, the stylus returned to its original starting position. The same stylus made the scratch on the sample surface. In the microscratch test, a normal load controlled conical indenter was driven into the gelatin/PET at a rate of 2 N/min and across the sample surface at a rate of 5 mm/min until failure events occurred in the sample. Once scratching was completed, another topographic scan (postscan) of the scratched surface was set up. The depth profile along the scratch track was defined as the difference between the postscan and prescan depths. After the sample was scratched, the morphology of the scratch track was observed by optical microscopy. Optical micrographs and depth profiles of the scratch track were used to evaluate the scratch morphology and failure mechanism.

Plasma treatment of PET

The 100 μm thick PET films used in this study were biaxially drawn untreated PET film purchased from the Shin-Kong Synthetic Fibers Corporation. Because of the high crystallinity (~40–50%) of the PET film from the drawing process, the surface of the PET film is generally difficult to adhere to without additional primer coating or energetic surface treatments. Plasma treatment or so-called glow discharge treatment is known to enhance the wettability of the treated surface, to produce reactive functional groups, and thus to improve the adhesion of layers coated on the surface. We used nitrogen plasma treatments to improve the adhesion between a PET substrate and a gelatin coating. A radiofrequency plasma treatment on PET film was performed with a nitrogen pressure of 200 mTorr, an output power of 40 W, and a radiofrequency of 13.56 MHz. We varied the duration of the plasma treatment (10, 100, and 200 s) to enhance the

adhesion between the PET surface and the gelatin film that was subsequently coated onto the PET. A high voltage electrode was fabricated from titanium metal and the ground aluminum electrode was the vacuum chamber itself. PET film samples were placed on a sample plate, which was located between the high voltage electrode and the ground electrode. This electrode and sample plate geometry provides greater uniformity of the treated surface of samples as verified by the contact angle measurement.

Surface analysis

Once the PET film is plasma treated, the film is quickly transferred into the chamber of an X-ray photoelectron spectroscopy (XPS) apparatus for measurement of the surface composition of the treated surfaces. The XPS spectra were acquired on a VG Scientific ESCALAB 250 photoelectron spectrometer with monochromatic Al Kα X rays (1486.6 eV). All spectra were referenced to the C 1s peak of the aliphatic carbon atoms, which was assigned a value of 284.6 eV. Spectra were taken at a 45° electron take-off angle, which roughly corresponds to an analysis depth of 5 nm. The surface elemental composition of the plasma-treated PET film is discussed later in the Results section.

Gelatin coating preparation

Gelatin powder was purchased from Showa Chemical Co. It was added to doubly distilled/deionized water and swelled at room temperature for at least 1 h. The mixture was heated to 60°C so that the powder completely dissolved in water to obtain a 10 wt % homogenous gelatin solution. The solution was coated on PET film immediately after the PET surface was plasma treated. All gelatin coatings were deposited on PET using surgical blades with different coating gap thicknesses to produce final dried gelatin coatings with thicknesses ranging from 10 to 100 μm. For coating the gelatin, PET film was first placed on a hot/cold plate. Because gelatin solution gels below 40°C, the surface temperature of the PET film must be maintained above 40°C during coating to produce a smooth surface. Once the gelatin was coated, the temperature of the hot/cold plate was quickly reduced to 15°C to form a gelatin gel for drying. The procedure of coating and drying of the gelatin layer follows Marshall and Petri.[21] During the drying process the single-stranded gelatin molecules can undergo a coil–helix transition to form partially renatured gelatin, and its mechanical properties depend on the amount of renatured gelatin. We used differential scanning calorimetry to characterize the amount of renatured gelatin and to verify the uniformity within each coating as well as different coatings.

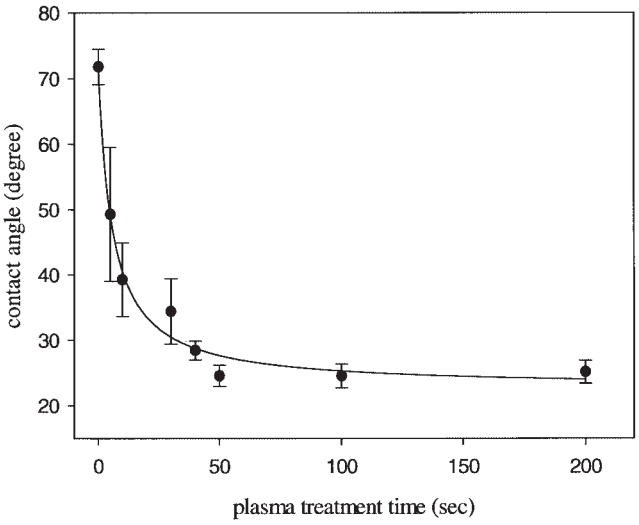

Figure 1 The contact angle of the water droplet on the plasma-treated surface of PET as a function of the treatment time. The plasma was generated under 200 mTorr nitrogen pressure and an output power of 40 W.

Gelatin is a highly moisture-sensitive biopolymer and its mechanical properties are greatly affected by the humidity of the testing environment. Therefore, it is important to control the temperature and the humidity of the gelatin/PET sample before and during the microscratch testing. The gelatin/PET samples were kept and tested under 60% relative humidity and a temperature of 25°C. Under these conditions, all film samples of gelatin/PET with different dried thicknesses of gelatin coating (~10–~50 μm) laid flat without any curl. This indicated that the gelatin/PET film samples were free of residual stresses resulting from the drying process. To avoid changes in the physical properties of the gelatin film, all samples were tested within 1 week of coating.

RESULTS AND DISCUSSION

The results of the scratch adhesion testing are divided into three different categories for discussion: the effect of the plasma treatment time, the effect of the annealing temperature, and the effect of the coating thickness.

Effect of plasma treatment time

The wetting properties and surface composition of PET were examined by contact angle measurements and XPS on the untreated and plasma-treated PET surfaces. As shown in Figure 1, the equilibrium contact angles of water on the untreated and plasma-treated PET film surfaces are plotted as a function of the plasma treatment time with a nitrogen pressure of 200 mTorr and 40-W output energy. With increasing plasma treatment time, the average contact angle de-

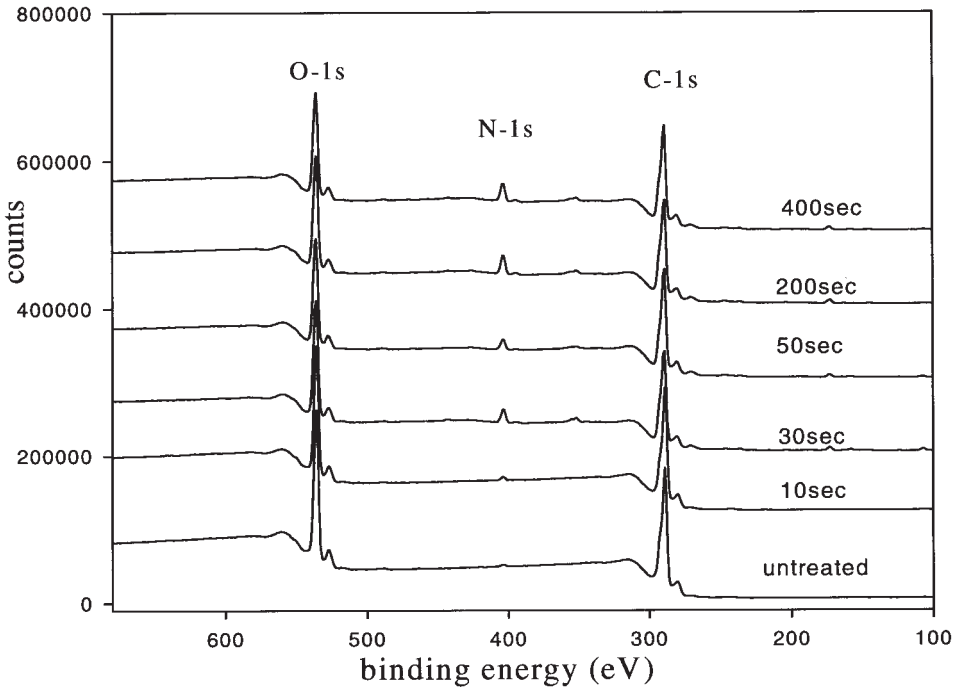

Figure 2 XPS survey spectra of biaxially oriented PET film plasma treated with increasing treatment times of (a) 0, (b) 10, (c) 30, (d) 50, (e) 200, and (f) 400 s.

creases quickly. For a treatment time of ≥50 s, the contact angle plateaus at a low value.

Detailed surface elemental compositions of untreated and treated PET film were revealed by XPS survey scan measurements as shown in Figure 2. PET is initially free of nitrogen. With increasing treatment time, PET shows an increase in the amount of nitrogen incorporation at the surface as seen from the growth of the N 1s peak. The ratio of the area under the C 1s peak to that of the N 1s peak, corrected for their ionization cross sections, provides the relative atom percentage of the nitrogen incorporation in the treated surfaces. Figure 3 shows that with increasing plasma treatment time the amount of nitrogen incorporation increases and levels off to a constant value of ~8% (N/C atom %) for a treatment time of ≥200 s. XPS

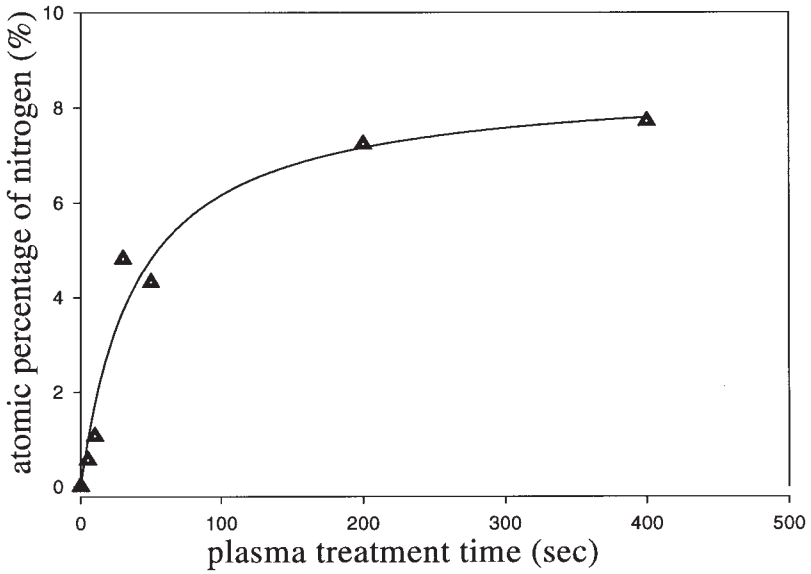

Figure 3 The atom percentage of nitrogen/carbon of the PET surface treated with nitrogen plasma as a function of the plasma treatment time. The atom percentage of the N/C ratio is plotted as a function of the plasma treatment time.

TABLE I
Surface Composition of PET Treated with N_2 Plasma for Different Treatment Times

Treatment time (s)	Composition of C 1s (%)				
	C—C	C—O	C═O	C—N	O═C—N
0	63.2	22.5	14.4	—	—
30	54.3	28.0	12.9	3.7	1.1
50	55.8	23.7	16.2	2.9	1.4
100	54.7	23.3	15.7	4.9	1.5
200	53.6	24.1	14.2	6.3	1.9
400	55.1	24.4	12.9	5.6	2.0

high-resolution spectra were also acquired to elucidate the chemical structure produced as a result of exposure of the PET surface to the nitrogen plasma treatment. The chemical compositions of the PET surface for different treatment times are listed in Table I. It shows that with increasing plasma treatment time both the number of amine (C—N signal) and amide (O═C—N signal) functional groups on the PET surface increases, with more of the amine groups than amide groups on the surface. For a treatment time of ≥200 s, the number of amine groups decreases slightly whereas the number of amide groups continues to increase. The increase of functional groups created on the PET surface can lead to a greater tendency for adhesion improvements after the gelatin solution is coated.

The PET films were plasma treated for 10, 100, and 200 s and coated with a gelatin layer of 50-μm dried thickness. The gelatin/PET samples were then annealed in an oven at 60°C for 2 h to promote adhesion between the gelatin and treated PET surface. Figure 4(a–c) provides optical micrographs of the scratch track morphology for the samples treated for 10, 100, and 200 s of nitrogen plasma, respectively. For a treatment time of 10 s [Fig. 4(a)], an interference pattern extending beyond the scratch track area was observed for a normal load of >1.6 N. The presence of this interference pattern indicates that a crack or a debond crack has formed between the gelatin coating and PET. In addition, for a normal load of >2.7 N, a clear scratch track is seen from the optical micrograph. For a plasma treatment time of 100 s, a scratch track area where gelatin debonded was also observed for a nor-

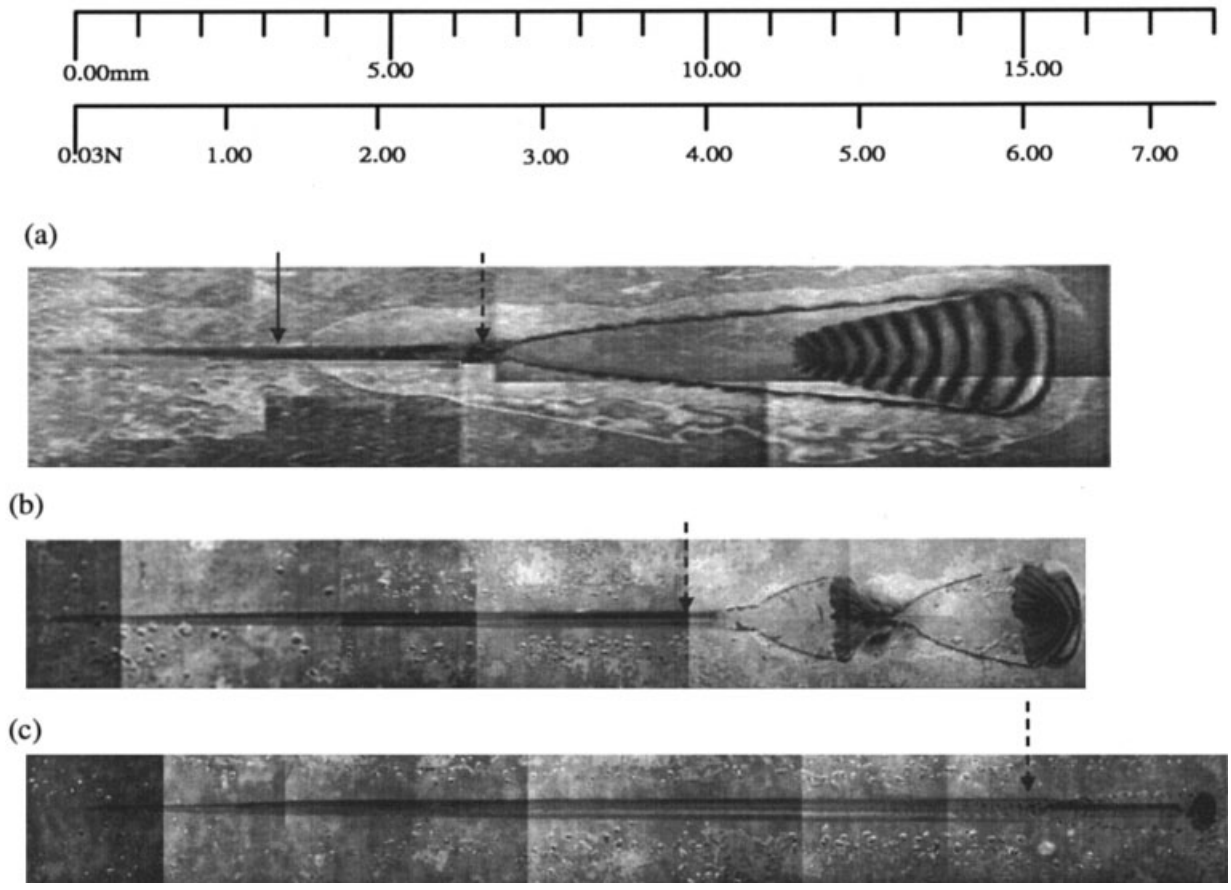

Figure 4 Optical micrographs of the scratch track morphology for plasma treatment for (a) 10, (b) 100, and (c) 200 s on the PET surface. The solid and dashed arrows indicate the locations at which coating detachment and coating removal failures occur, respectively.

mal load of >4.0 N [Fig. 4(b)]. For a 200-s plasma treatment time, the normal load at which the track clearance occurred is shown in Figure 4(c) for a normal load of >5.9 N.

Based on these observed failure morphologies, we define the F_c as the normal load at which the gelatin coating is detached but remains on the PET substrate surface to create an appearance of an interference pattern or the normal load at which the gelatin coating is removed or plowed to show a clear scratch track. For a 10-s plasma treatment, we observed both debonding failure at an F_c of 1.6 N and coating removal failure at an F_c of 2.7 N. For 100- and 200-s plasma treatments, we observed coating removal failure at F_c values of 4.0 and 5.9 N, respectively. From Figure 4(a–c) we observe that the failure morphologies changed from a combination of both debonding and coating removal failures to a one-mode failure of only coating removal failure with an increase in F_c to failure. The increase in the critical load with increasing treatment time is consistent with the result that the amount of nitrogen incorporation increases with increasing treatment time. As the plasma treatment time on the PET surface increases, it is expected that adhesion between the gelatin coating and treated PET surface increases as the gelatin coating reacts with the functional groups on the PET surface generated by the plasma treatment. The critical load increases as the adhesion is enhanced. The result supports that the critical load obtained from the scratch measurement can be used to evaluate coating adhesion.

The normal load, tangential load, and depth profile versus the scratch length of the samples used in Figure 4 are plotted in Figure 5(a–c), respectively. The data for different treatment times in each part are offset from each other to avoid overlap. The arrows shown in the figure indicate the locations along the scratch length at which detachment (solid arrow) or coating removal (dashed arrow) failure mechanisms were observed from the optical micrographs shown in Figure 4. As previously discussed in the Experimental section, the microscratch device used in this study is a normal load controlled device. Therefore, the normal load curves shown in Figure 5(a) were programmed to increase linearly with the scratch length at a rate of 0.4 N/mm. The corresponding tangential load curve showed a general increasing trend with increasing scratch length superposed with load oscillations. However, the location of detachment or coating removal failure observed from the optical micrograph does not appear to match the onset of oscillation. This observation is in contrast with the results obtained from several other studies in which load drops, load oscillations, or acoustic emissions correlated with fracture in hard coating/substrate systems.[20,22,23] This observation may be the result of the lower modulus and larger plastic deformation properties of softer polymer/polymer systems. During scratching, the indenter induces a large elastic and plastic deformation. The elastic deformation, however, recovers when the

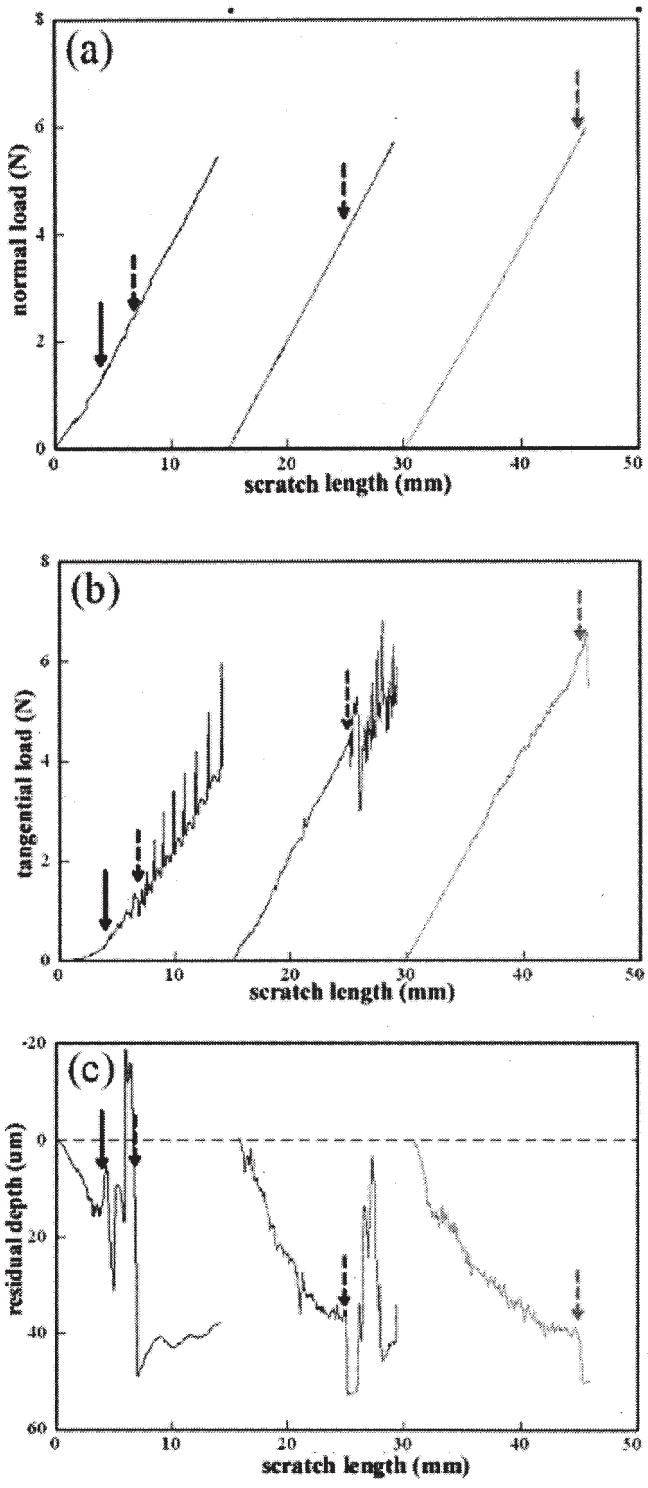

Figure 5 (a) The normal load, (b) tangential load, and (c) depth profile are plotted as a function of the scratch length of the samples treated with 10, 100, and 200 s of plasma. The solid and dashed arrows indicate the location at which coating detachment and coating removal failures occur, respectively.

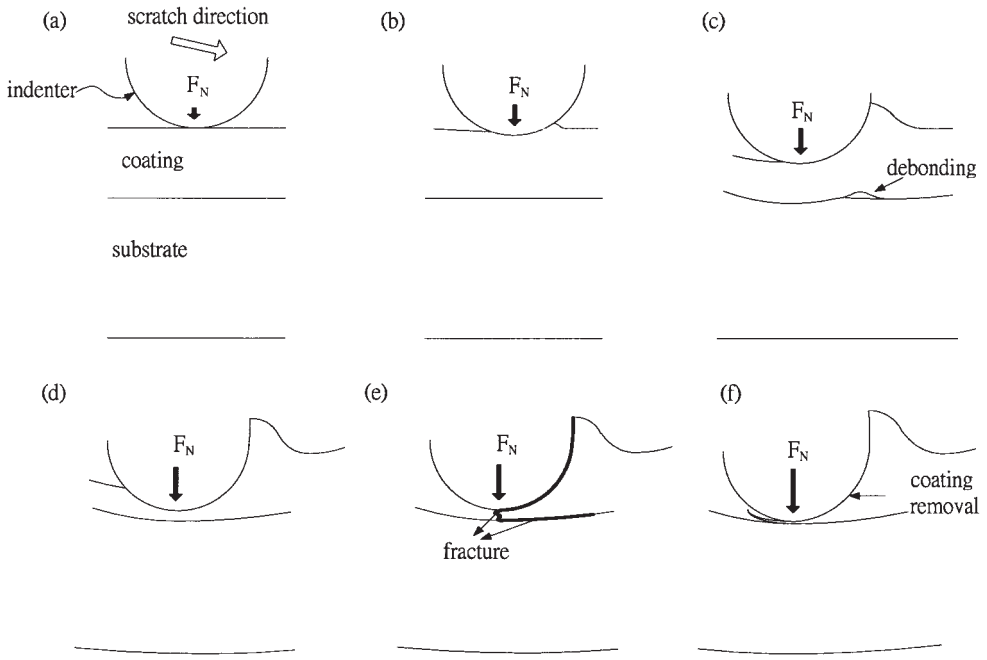

Figure 6 A schematic diagram showing indenter and coating/substrate interactions during scratching.

load is removed. The depth profile of the scratch track is plotted in Figure 5(c). For a 10-s plasma treatment time, the gelatin coating debonds from the PET substrate roughly at a depth of ~20 μm (solid arrow), which is less than one-half of the gelatin coating thickness of 50 μm. The dashed arrow indicates the location at which complete coating removal failure occurs. The depth at which the coating started to be removed is roughly equal to the coating thickness. For treatment times of 100 and 200 s, similar trends were observed and there was a sudden drop in the depth profile at which the gelatin coating was abruptly sheared off and removed from the PET. In general, the scratch track deformation resulted from the plastic deforma-

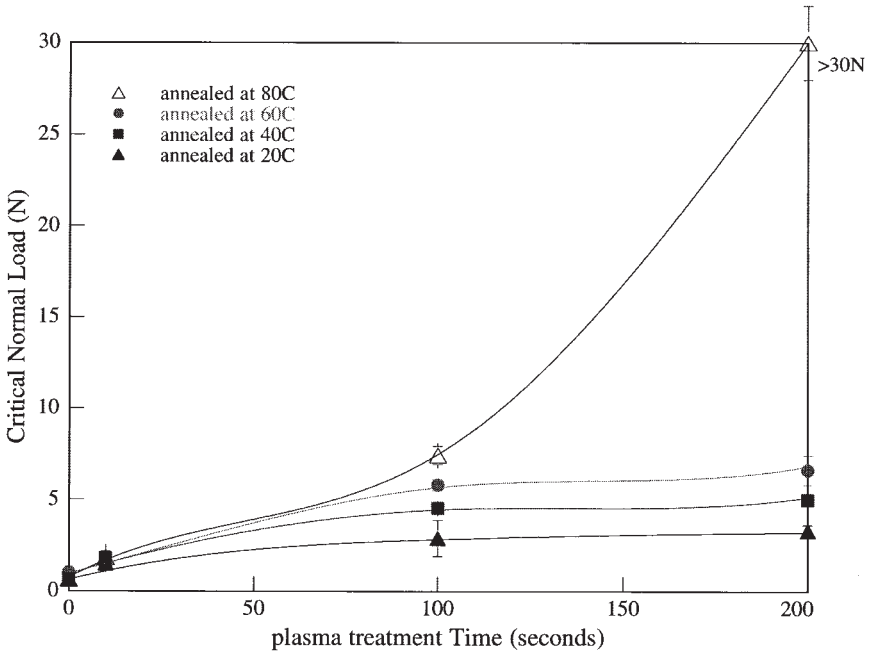

Figure 7 The critical load is plotted as a function of plasma treatment, in which the effect of the heat treatment temperature on the critical load is examined.

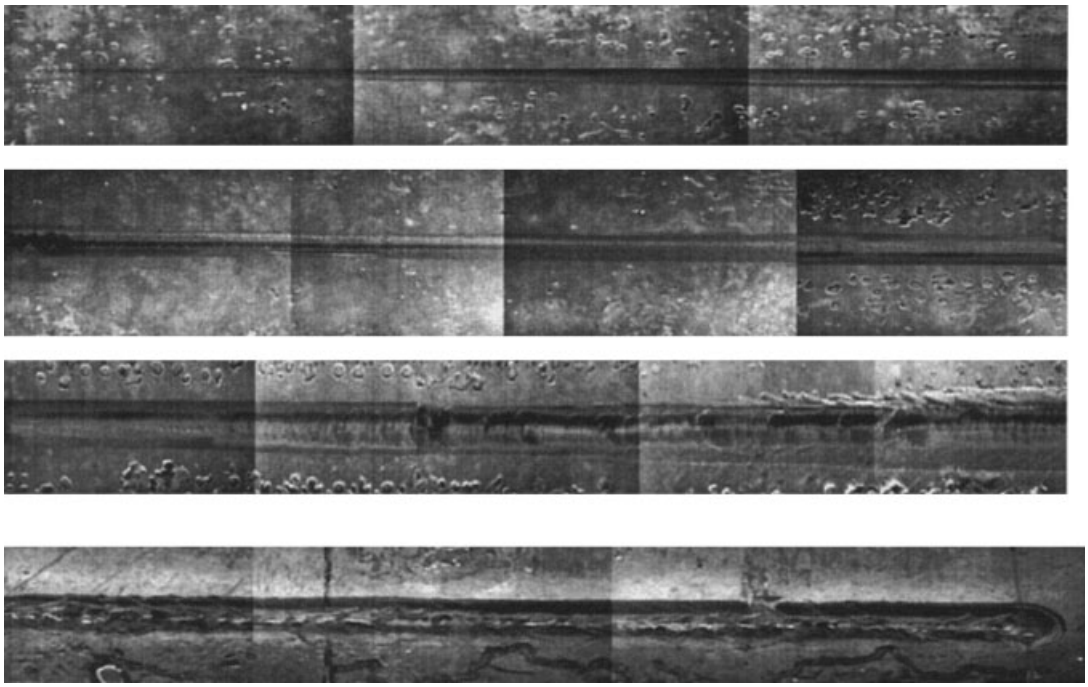

Figure 8 An optical micrograph of the scratch track morphology for a sample treated with 200 s of plasma and subsequently annealed at 80°C for 2 h. No coating detachment and coating removal failures are observed during scratching.

tion, pile-up, and wear of the coating/substrate. If the coating removal failure resulted only from the wear of the coating/substrate material from the scratching process, then a continuous depth profile would be expected. The sharp drop in the depth profile indicated that the coating removal failure occurred when the shear stress induced from the indenter exceeded the interfacial shear strength and break strength of the

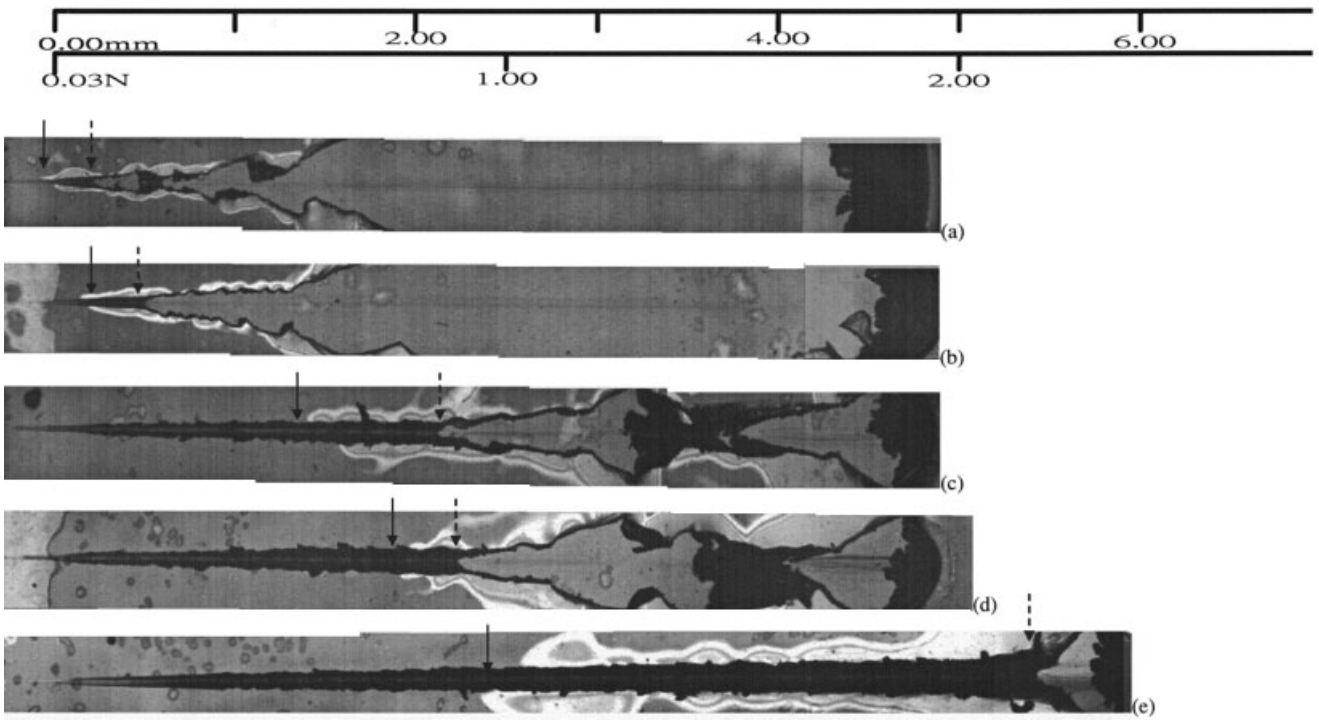

Figure 9 Optical micrographs of the scratch track morphology for samples without any plasma treatment. The thicknesses of the gelatin coatings are (a) 10, (b) 15, (c) 20, (d) 30, and (e) 45 μm.

gelatin coating. Therefore, the F_c for coating removal is a complex parameter, which is related to the adhesion.

Based on these results, a general indenter and coating/substrate interaction is proposed. A schematic diagram of the indenter–polymer interactions producing a scratch is shown in Figure 6(a–f). Initially, the indenter creates plastic deformation, wear, and pile-up on the coating/substrate sample. As the load increases above F_c, the maximum shear stress occurring beneath the indenter exceeds the shear strength of the interface. Detachment of the coating then results [Fig. 6 (c)]. The detachment of the coating is consistent with the work proposed by O'Sullivan and King,[17] who showed that Von Mises stress discontinuity increased with increasing normal load. With further increases in the normal load and therefore increases in the penetration depth of the indenter, greater plastic deformation of coating/substrate is produced. Such large plastic deformation can cause fracture of the coating, which results in the abrupt removal of the coating from the substrate [Fig. 6(e)]. The maximum stress acting on the surface of the indenter tip is such that the indenter rides up over the pile-up material. Note that the coating detachment mechanism occurs at a lower load than that required for scratch track clearance. As the stress built up in front of the moving indenter, a crack initiated at the bottom of the tip and propagated first into the gelatin coating and later into the gelatin/PET interface to induce the coating removal failure.

Effect of annealing temperature

We examined the effect of the heat treatment temperature on the adhesion of gelatin/PET samples. The samples were prepared by first treating the PET surface with nitrogen plasma at a 40-W output power, coating a 50-μm gelatin on the treated PET surface and heat treating the gelatin/PET sample at different annealing temperatures for 2 h. Figure 7 plots the critical normal load as a function of the plasma treatment time for samples heat treated at 20, 40, 60, and 80°C. There is a general trend that with increasing treatment time the critical load increases and reaches a plateau critical load for a treatment time of $>$50 s, except for samples treated at 80°C, in which case the critical load increases exponentially. With increasing heat treatment temperature, the critical load increases for all plasma treatment times. These results support the conclusion from the previous section that there is a chemical reaction between the gelatin coating and functionalized PET surface. Moreover, the critical load can be used qualitatively to evaluate the adhesion. For samples plasma treated for 200 s and heat treated at 80°C, coating detachment and coating removal failures are not observed up to the (equipment) maximum load of 30 N. For a normal load of 30 N, the indenter penetrated through the gelatin coating and created a large plastic deformation in the PET film. However, no sign of interfacial failures were observed. The corresponding optical micrograph is shown in Figure 8.

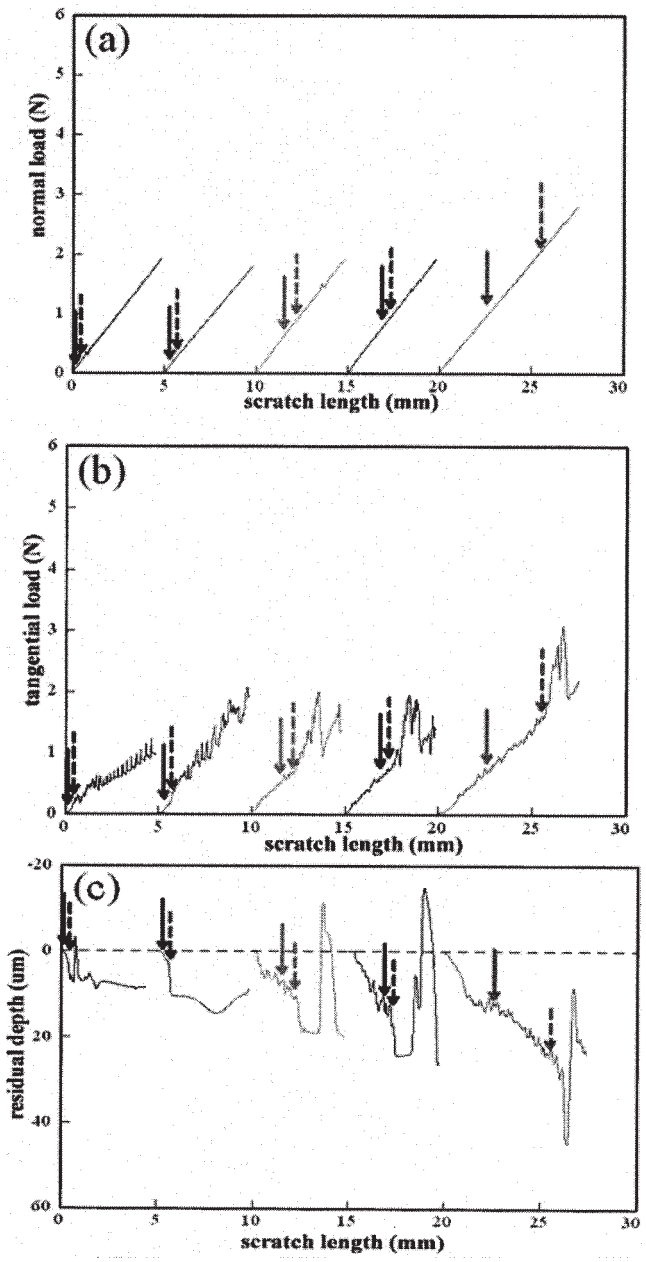

Figure 10 (a) The normal load, (b) tangential load, and (c) depth profile are plotted as a function of the scratch length of the samples used in Figure 9.

Effect of gelatin coating thickness

The effects of the gelatin coating thickness on the critical load and failure mechanism of gelatin/PET treated with 0, 10, 100, and 200 s of plasma were examined. The optical micrographs in Figure 9(a–e) show the scratch track morphology of untreated samples with different gelatin thicknesses ranging from 10

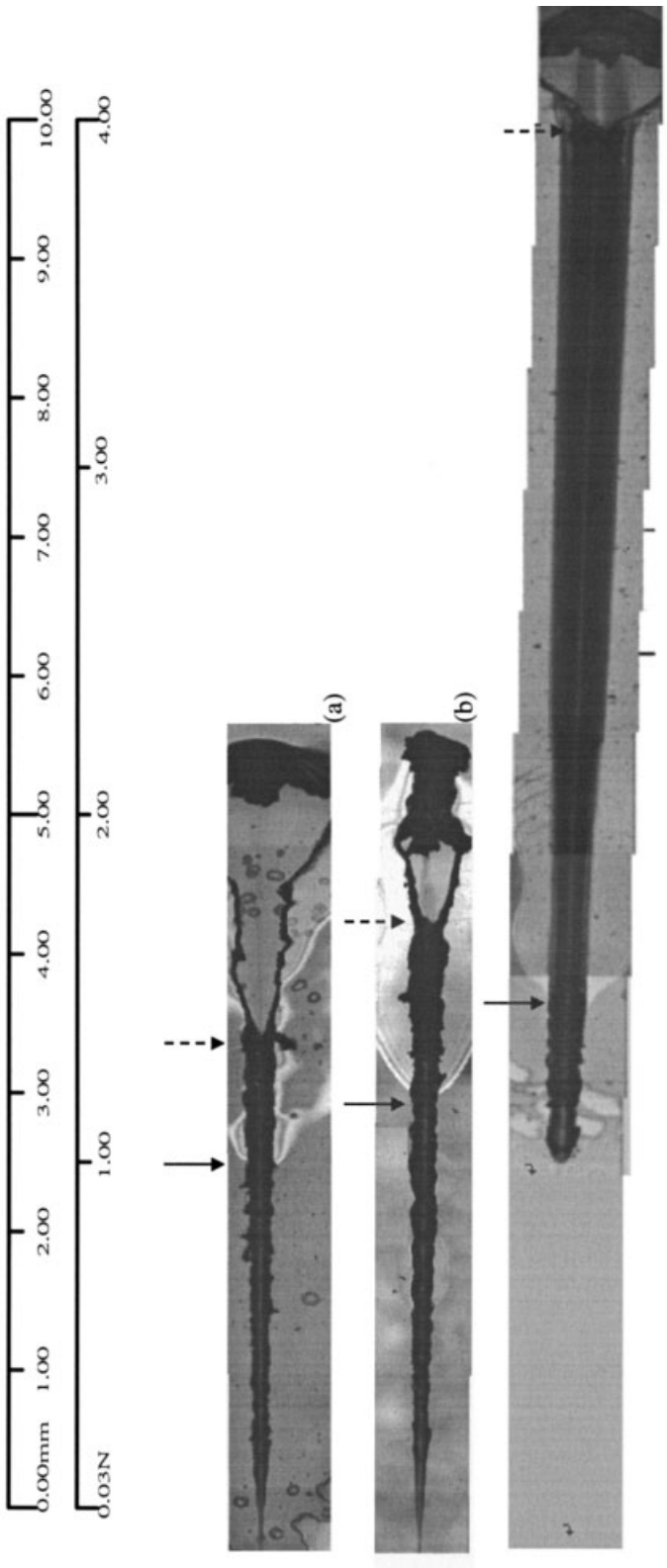

Figure 11 Optical micrographs of the scratch track morphology for samples with 10-s plasma treatment. The thicknesses of the gelatin coatings are (a) 12, (b) 25, and (c) 50 μm.

to 50 μm. The solid arrows indicate the location where the gelatin coating detached from the PET substrate. The dashed arrows indicate the locations where the gelatin coating was completely removed from the PET surface. We found that the F_c (detachment) increased roughly linearly with increasing thickness. The F_c (coating removal) increased more strongly with the gelatin coating thickness. Because the PET used in all samples was untreated, the work of adhesion between the gelatin coating and PET substrate was the same for gelatin coatings of different thicknesses. However, the dependence of the F_c on the coating thickness demonstrates that both film detachment and coating removal failures depend not only on the adhesive properties but also on the plastic deformation of the coating and substrate. The critical load for coating removal shows a stronger dependence on the coating thickness than that for the coating detachment because the coating removal failure requires a certain minimum extent of plastic deformation in the coating/substrate before the coating is fractured.

Figure 10(a–c) plots the corresponding normal load, tangential load, and depth profile as a function of the scratch length. The location of coating detachment and coating removal failures that were revealed from the optical micrographs do not appear to correlate with the position at which the normal and tangential load started oscillating. With increasing normal and tangential loads, the general trend for each depth profile increased because of the plastic deformation and wear and pile-up of coating/substrate material. All samples showed both coating detachment and coating removal failures. In addition, the coating detachment failure preceded the coating removal failure. The depth at which film detachment occurs is well above the gelatin/PET interface. For the coating removal failure, there was an abrupt drop in the depth profile, which indicated a sudden shearing of the coating from the PET substrate. The depth after which the gelatin coating was removed roughly corresponds to the original thickness of the gelatin coating. Occasionally, large plastic deformation created build-up of material in the scratch track, which caused the observed increase in the depth profile.

The effect of the coating thickness on the scratch adhesion behavior can be further examined for PET substrates treated with 10 s of nitrogen plasma. The optical micrographs in Figure 11 show the scratch morphology of samples with gelatin thicknesses of 12, 25, and 50 μm. Similar to the samples without any plasma treatment, all samples treated for 10 s showed both coating detachment and coating removal failures. For 50-μm gelatin coatings, scratching started from a normal load of 1 N instead of from the typical minimum normal load of 0.03 N. We found that the normal load starting position did not affect the final scratch behavior as long as it was smaller than the critical load

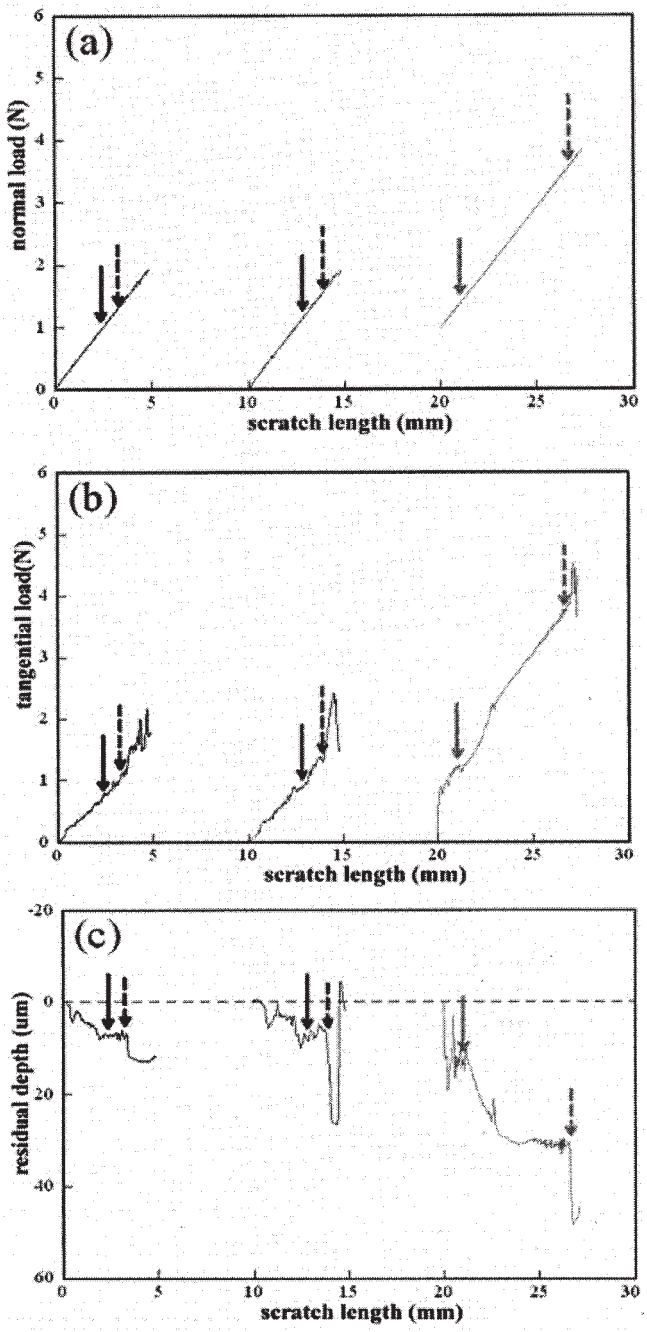

Figure 12 (a) The normal load, (b) tangential load, and (c) depth profile are plotted as a function of the scratch length of the samples used in Figure 11.

for both failure mechanisms. This was verified by a scratch test starting from the minimum normal load (not shown) on the same sample. No change in the failure mechanism and the corresponding critical load was observed. The load at which coating detachment occurred increased roughly linearly with increasing thickness, whereas the critical load for coating removal showed greater dependence on the coating thickness, as seen before. Therefore, the F_c is not only a function of the adhesive property but also a complex

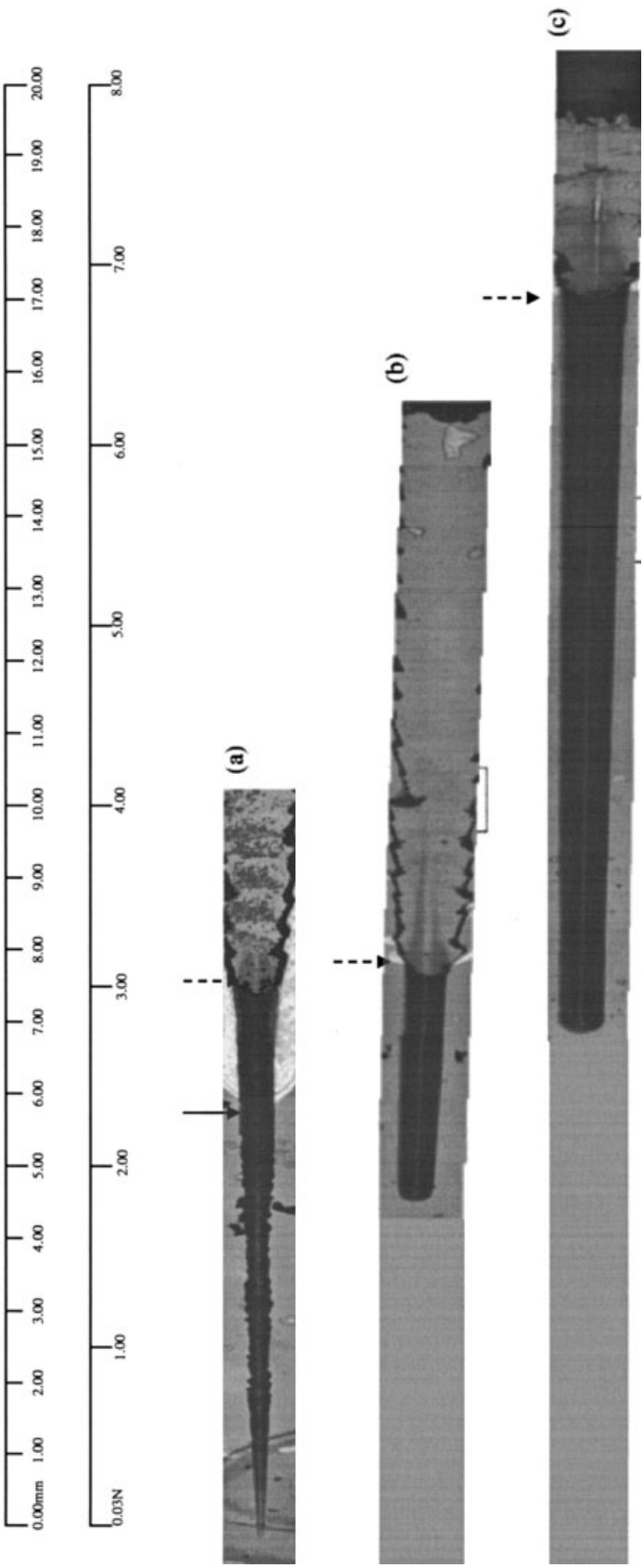

Figure 13 Optical micrographs of the scratch track morphology for samples with 200-s plasma treatment. The thicknesses of the gelatin coatings are (a) 12, (b) 25, and (c) 50 μm.

function of the mechanical and fracture properties of the coating.

The normal load, tangential load, and depth profile are plotted as a function of the scratch length for 10-s plasma treatment samples in Figure 12(a–c). From the depth profile, we observed that coating detachment failure occurred at a relatively shallow penetration depth compared to the thickness of the coating. For coating removal failure, an abrupt change in the depth profile was always observed.

We only discuss the results from 200-s plasma treatment (Figs. 13, 14), because a similar trend was observed for samples treated with 100 s of plasma. For a 12-μm coating thickness, we observed critical loads for coating detachment and coating removal at 2.4 and 3.0 N, respectively. For thicknesses of 25 and 50 μm, only coating removal failure is observed at critical loads of 3.2 and 6.8 N, respectively. It appeared that coating detachment failures did not occur for 25 and 50 μm of gelatin coating. However, it is possible that both failures occurred simultaneously at the same load and that only the coating removal failure was observed because the coating removal failure makes the interference pattern resulting from the coating detachment failure disappear. Because the coating detachment failure was caused by the stress field underneath the indenter tip, the thicker the coating was, the deeper the indenter needed to penetrate into the sample to cause coating detachment. Therefore, the critical load for coating detachment increased with increasing thickness and the coating detachment failure may merge with the coating removal failure.

The thicknesses of the coating as well as the plasma treatment conditions affect the critical load at which coating detachment and coating removal failures occur. These effects are summarized and shown in Figure 15. The critical load is plotted as a function of the coating thickness for samples treated with 0, 10, 100, and 200 s of nitrogen plasma and subsequent heating treatment at 60°C for 2 h. For untreated samples, the critical load for coating detachment increased linearly with increasing gelatin thickness up to 100-μm thickness gelatin. For samples plasma treated for 10 s, similar linearity was found for coating thicknesses greater than 50 μm. However, for thicknesses less than 50 μm, the critical load for samples treated with 10 s of plasma is greater than that for the untreated samples of the same thickness. For samples treated for 100 and 200 s, the critical load increased exponentially with increasing coating thickness. The failure mechanism also changed from coating detachment failure for thin coatings to coating removal failure for thick coatings. We expected that with increasing plasma treatment time the adhesion between the coating/substrate would improve. For samples of the same coating thickness, the F_c increased with increasing treatment time. This result was consistent with the XPS results,

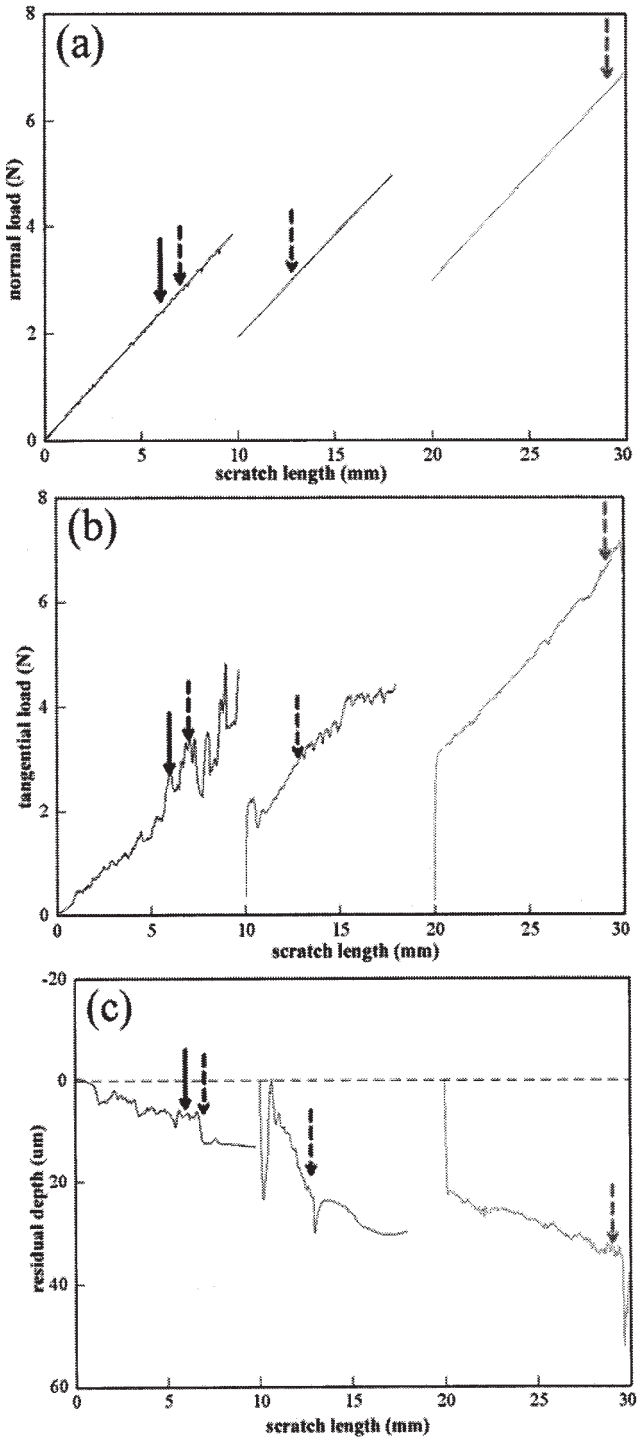

Figure 14 (a) The normal load, (b) tangential load, and (c) depth profile are plotted as a function of the scratch length of the samples used in Figure 13.

which showed that surface functionalization increased with increasing treatment time. In addition, as the adhesion was improved with increasing treatment time, coating detachment failure could be completely suppressed and replaced with the coating removal failure during scratching. Therefore, for thicker coat-

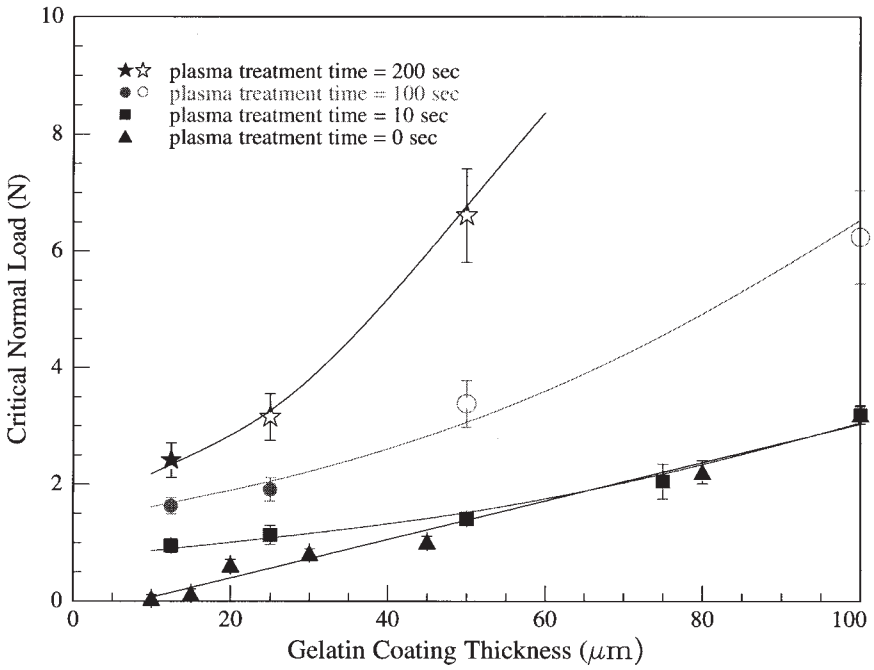

Figure 15 The critical normal load versus gelatin coating thickness for different plasma treatment times. Solid symbols correspond to coating detachment and open symbols correspond to coating removal.

ings, the F_c was a complex function of the coating thickness, the mechanical properties of the coating/substrate, and the adhesion properties between the coating and substrate.

As the thickness of the coating decreased, the plastic deformation in the coating caused by scratching decreased and the energy was mainly dissipated in fracturing the interface and in the deformation the PET substrate. For $<$50-μm coating thickness, the critical load was independent of the coating thickness and the critical load increased with increasing plasma treatment time. In another hard coating/substrate system, similar scratch adhesion results were obtained.[24] Therefore, as the coating thickness decreased, the relative interfacial strength could be assessed with the relative value of the critical normal load. Note that in our study a 50-μm radius indenter was used. It appears that a larger indenter radius to coating thickness ratio allows the F_c to be a qualitative parameter to evaluate adhesion. The effect of the indenter radius on the scratch adhesion behavior will be examined in future work.

CONCLUSION

We used a microscratch technique to evaluate the adhesion between a gelatin coating and a PET surface treated with nitrogen plasma. The failure mechanism and the critical load were dependent on the complex interactions between the indenter and the coating/substrate system, which included the ratio between the indenter tip radius and the coating thickness, the hardness ratio between the coating and substrate, the mechanical properties of the coating/substrate, and the interfacial adhesion. For the current system, the failure mechanism characteristics are summarized as follows:

1. Coating detachment failure occurred at relatively low load as the indenter penetrated into the coating at a depth of roughly less than one-half of the coating thickness.
2. Coating removal failure occurred at higher load than coating detachment failure. The failure occurred when the indenter penetrated close to the interface.
3. The F_c was affected by both the coating thickness and the interfacial adhesion.
4. For a thin coating (compared with the indenter radius), the F_c was found to be closely related to adhesion; therefore, it could be used to qualitatively compare adhesion of polymer layer materials.

This work is supported by the National Science Council and the Ministry of Economics of Taiwan.

References

1. Myers, R. R.; Long, J. S., Eds. Treatise on Coatings; Marcel Dekker: New York, 1975.

2. Tunstall, A.; Eberhart, R. C.; Prager, M. D. J Biomed Mater Res 1994, 28, 1233.
3. Hsu, S.-H.; Chen, D. C. U.S. Pat. 6,579,322 (2003).
4. Laemmel, E.; Penhoat, J.; Warocquier-Clerout, R.; Sigot-Luizard, M.-F. J Biomed Mater Res 1998, 39, 446.
5. Rose, P. I. In The Theory of the Photographic Process, 4th ed.; James, T. H., Ed.; Macmillan: New York, 1977; p 51.
6. Lavielle, L.; Schultz, J.; Nakajima, K. J Appl Polym Sci 1991, 42, 2825.
7. Mittal, K. L., Ed. Adhesion Measurement of Thin Films, Thick Films and Bulk Coatings; American Society for Testing and Materials: Philadelphia, 1976.
8. Marshall, D. B.; Evans, A. G. J Appl Phys 1984, 56, 2632.
9. Wu, T. W. J Mater Res 1991, 6, 407.
10. Matthewson, M. J Appl Phys Lett 1986, 49, 1426.
11. Ritter, J. E.; Lardner, T. J.; Rosenfeld, L.; Lin, M. R. J Appl Phys 1989, 66, 3626.
12. Hertz, H. In Miscellaneous Papers by H. Hertz; Schott, J. Ed.; Macmillan: London, 1896.
13. Johnson, K. L. Contact Mechanics; Cambridge University Press: Cambridge, UK 1985.
14. Steinmann, P. A.; Hintermann, J. J Vac Sci Technol 1985, A3, 2394.
15. Valli, J.; Makela, V.; Mattews, A. Surf Eng 1986, 2, 49.
16. Ichimura, H.; Rodrigo, A. Surf Coat Technol 2000, 126, 152.
17. O'Sullivan, T. C.; King, R. B. J Tribol 1988, 110, 235.
18. Malzbender, J.; de With, G. Surf Coat Technol 2002, 154, 21.
19. Liu, A.; Sun, J.; Shen, W. Tribol Int 2002, 35, 511.
20. Ichimura, H.; Ishii, Y. Surf Coat Technol 2003, 165, 1.
21. Marshall, A. S.; Petrie, S. E. B. J Photogr Sci 1980, 28, 128.
22. Venkataraman, S. K.; Kohlstedt, D. L.; Gerberich, W. W. J Mater Res 1992, 7, 1126.
23. Bull, S. J. Surf Coat Technol 1991, 50, 25.
24. Venkataraman, S. K.; Nelson, J. C.; Hsieh, A. J.; Kohlstedt, D. L.; Gerberich, W. W. J. Adhes Sci Technol 1993, 7, 1279.